



JLAB-THY-08-849
NT@UW-08-13
UMD-40762-414

Kaon Condensation with Lattice QCD

William Detmold,¹ Kostas Orginos,^{2,3} Martin J. Savage,¹ and André Walker-Loud^{2,4}

(NPLQCD Collaboration)

¹*Department of Physics, University of Washington, Seattle, WA 98195-1560.*

²*Department of Physics, College of William and Mary, Williamsburg, VA 23187-8795.*

³*Jefferson Laboratory, 12000 Jefferson Avenue, Newport News, VA 23606.*

⁴*Department of Physics, University of Maryland, College Park, MD 20742-4111.*

(Dated: October 25, 2018)

Abstract

Kaon condensation may play an important role in the structure of hadronic matter at densities greater than that of nuclear matter, as exist in the interior of neutron stars. We present the results of the first lattice QCD investigation of kaon condensation obtained by studying systems containing up to twelve negatively charged kaons. Surprisingly, the properties of the condensate that we calculate are remarkably well reproduced by leading order chiral perturbation theory. In our analysis, we also determine the three-kaon interaction from the multi-kaon systems and update our results for pion condensates.

arXiv:0807.1856v1 [hep-lat] 11 Jul 2008

I. INTRODUCTION

A key ingredient in determining whether supernovae evolve into black-holes or neutron stars is the nuclear equation of state (NEOS) [1]. The NEOS depends upon the degrees of freedom at a given density, which in turn are determined by the masses of the various hadrons in the medium and their interactions. One possibility is that it is more energetically favorable for a Bose-Einstein condensate of negatively charged mesons to form in the hadronic matter. Naively, one expects pion condensation to occur before kaon condensation¹, however, the repulsive pion-nucleon interactions and the attractive kaon-nucleon interaction lead to kaon condensation being the prime candidate for softening the NEOS at moderate nuclear densities. In theoretical explorations of kaon condensation, chiral perturbation theory (χ PT) is used to describe the kaon-nucleon interactions and the kaon self-interactions at leading order (LO) or next-to-leading order (NLO) in the chiral expansion [4]. The energy of the hadronic plus electronic system is minimized with respect to the vacuum expectation values (the condensates) of the meson fields subject to the constraints imposed by charge neutrality and the conservation of baryon number. In the case of non-interacting mesons, once the chemical potential exceeds the rest mass of a given species of meson a condensate will form with an infinite density of mesons. However, in the case of a meson with repulsive self-interactions, the number density of mesons will remain finite and a smooth function of the chemical potential. Depending upon the many-body technique employed to describe the system, a condensate of K^- 's may become energetically favorable at baryon densities, n_b , as low as three times nuclear matter density (for a nice discussion, see ref. [2]).

In this work we perform the first Lattice QCD studies of kaon condensation. In particular, we calculate the correlation functions of systems containing up to twelve ($n = 12$) K^- 's on the coarse MILC lattices with spatial extent $L \sim 2.5$ fm and $L \sim 3.5$ fm, both with lattice spacing $b \sim 0.125$ fm, and on the fine MILC lattices with spatial extent $L \sim 2.5$ fm and lattice spacing $b \sim 0.090$ fm. LO χ PT is found to describe the chemical potential, and its density dependence, remarkably well over the densities explored. This work is an extension of our previous work on charged-pion condensates [5, 6] and, for completeness, we update that analysis with the new ensembles studied herein.

II. CONDENSATION OF PSEUDO-GOLDSTONE BOSONS IN χ PT

At LO in χ PT, the Lagrange density describing the low-energy dynamics of the pseudo-Goldstone bosons associated with the spontaneous breaking of the approximate $SU(3)_L \otimes SU(3)_R$ chiral symmetry of QCD has the form

$$\mathcal{L} = \frac{f^2}{8} \text{Tr} [\partial_\mu \Sigma \partial^\mu \Sigma^\dagger] + \lambda \text{Tr} [m_q (\Sigma + \Sigma^\dagger)] \quad , \quad (1)$$

¹ A second possibility is that it is energetically favorable to have Σ^- 's present in the nuclear material in addition to neutrons and protons. The in-medium mass of the Σ^- is expected to be significantly less than in free-space due to its interactions with neutrons, but the precise mass-shift is uncertain due to the model dependence of existing theoretical calculations [2]. Experimentally, little is known about the Σ^- -neutron interaction and a precise Lattice QCD calculation of these interactions [3] would greatly reduce the uncertainty in this particular contribution to the NEOS.

where Σ is the exponential of the meson fields,

$$\Sigma = e^{i2M/f} \quad , \quad M = \begin{pmatrix} \frac{1}{\sqrt{2}}\pi^0 + \frac{1}{\sqrt{6}}\eta^0 & \pi^+ & K^+ \\ \pi^- & -\frac{1}{\sqrt{2}}\pi^0 + \frac{1}{\sqrt{6}}\eta^0 & K^0 \\ K^- & \bar{K}^0 & -\frac{2}{\sqrt{6}}\eta^0 \end{pmatrix} \quad , \quad (2)$$

and where f is the chiral limit of the pion decay constant (in this normalization convention the physical pion decay constant is $f_\pi \sim 132$ MeV). At LO in the chiral expansion, the quark mass matrix, m_q , can be written in terms of the meson masses,

$$\lambda m_q = \frac{f^2}{8} \begin{pmatrix} m_\pi^2 & 0 & 0 \\ 0 & m_\pi^2 & 0 \\ 0 & 0 & 2m_K^2 - m_\pi^2 \end{pmatrix} \quad . \quad (3)$$

The Lagrange density in eq. (1), in addition to describing the free-field dynamics of the mesons, also contains interactions containing arbitrary numbers of mesons. At zero momentum, the LO contributions to the interactions between three charged pions or between three charged kaons are given by

$$\mathcal{L} = \frac{2}{3f^4} [m_\pi^2(\pi^+)^3(\pi^-)^3 + m_K^2(K^+)^3(K^-)^3] \quad . \quad (4)$$

This contribution provides the naive dimensional analysis (NDA) estimate of the size of the three-meson interaction [7, 8] of $1/(m_\pi f^4)$ for the $\pi^-\pi^-\pi^-$ interaction and $1/(m_K f^4)$ for the $K^-K^-K^-$ interaction in the non-relativistic theory describing the very-low momentum interactions between the mesons ².

In the presence of a chemical potential for the third component of isospin, μ_I , and strangeness, μ_S , the partial derivatives in eq. (1) become covariant derivatives [9, 10, 11]

$$\partial_\mu \Sigma \rightarrow D_\mu \Sigma = \partial_\mu \Sigma + i\delta_{\mu 0} \mu_I [\hat{I}_z, \Sigma] + i\delta_{\mu 0} \mu_S [\hat{S}, \Sigma] \quad , \quad (5)$$

where

$$\hat{I}_z = \frac{1}{2} \begin{pmatrix} +1 & 0 & 0 \\ 0 & -1 & 0 \\ 0 & 0 & 0 \end{pmatrix} \quad , \quad \hat{S} = \begin{pmatrix} 0 & 0 & 0 \\ 0 & 0 & 0 \\ 0 & 0 & +1 \end{pmatrix} \quad . \quad (6)$$

In the situation where $\mu_{\pi^-} = -\mu_I > m_\pi$ and $\mu_{K^-} = \mu_S - \frac{1}{2}\mu_I < m_K$, it is energetically favorable to form a π^- condensate but not a K^- condensate, and at LO in χ PT the number density of π^- 's is [9, 10]

$$\rho_{\pi^-} = \frac{f_{\pi^-}^2}{2} \left(\mu_{\pi^-} - \frac{m_\pi^4}{\mu_{\pi^-}^3} \right) \quad . \quad (7)$$

The analysis leading to this result easily extended to kaon-condensates [11]. For $\mu_{\pi^-} < m_\pi$ and $\mu_{K^-} > m_K$ there will be a condensate of K^- 's but not of π^- 's ³. For chemical potentials

² The relativistic and non-relativistic fields differ in their normalization by a factor of \sqrt{m} .

³ Mixed states with different numbers of pions and kaons are the subject of ongoing work.

in this range, the number density of K^- 's as a function of the chemical potential, μ_{K^-} , is, at LO in χ PT,

$$\rho_{K^-} = \frac{f_{K^-}^2}{2} \left(\mu_{K^-} - \frac{m_K^4}{\mu_{K^-}^3} \right) . \quad (8)$$

In eqs. (7) and (8), we have used LO χ PT relations to express the result in terms of the physical masses and decay constants. It is this relation that we will compare with Lattice QCD calculations. The reason for “testing” the relation in eq. (8) is that, given the relatively large expansion parameters of $SU(3)_L \otimes SU(3)_R$ χ PT, it is natural to expect that there will be corrections to ρ_{K^-} , and hence to the dependence of μ_{K^-} on ρ_{K^-} , at the level of $m_K^2/\Lambda_\chi^2 \sim 25\%$, where $\Lambda_\chi \sim 1$ GeV is the scale of chiral symmetry breaking.

In order to assess the relevance of the present work, it is instructive to compare the value of the K^- -condensates we calculate to those found to be relevant to the dense nuclear matter in the interior of neutron stars. Decomposing the charged kaon fields into their real and imaginary parts, $K^\pm = (K_1 \mp iK_2)/\sqrt{2}$, and denoting the condensates $\langle K_1 \rangle = v_1$ and $\langle K_2 \rangle = v_2$ and further defining $\langle K \rangle = \sqrt{v_1^2 + v_2^2}/\sqrt{2}$, the condensate is related to the chemical potential via

$$\frac{\langle K \rangle}{f_K} = \frac{1}{2} \cos^{-1} \left(\frac{m_K^2}{\mu_{K^-}^2} \right) . \quad (9)$$

Condensates of magnitude $\langle K \rangle/f_K \lesssim 0.3$ are found to be possible at the densities in the interior of neutron stars [4]. This corresponds to $\mu_{K^-}/m_K - 1 \lesssim 0.1$, which is contained in the region explored in the Lattice QCD calculations described in this work.

III. MULTI-MESON ENERGIES IN A FINITE VOLUME

In recent works [7, 8, 12], the analytic volume dependence of the ground-state energy of n identical bosons in a periodic volume of side L has been computed to $\mathcal{O}(L^{-7})$, extending the classic results of Bogoliubov [13] and Lee, Huang and Yang [14]. The resulting shift in ground-state energy of n particles of mass M due to their interactions is [8]

$$\begin{aligned} \Delta E_n = & \frac{4\pi \bar{a}}{M L^3} {}^n C_2 \left\{ 1 - \left(\frac{\bar{a}}{\pi L} \right) \mathcal{I} + \left(\frac{\bar{a}}{\pi L} \right)^2 [\mathcal{I}^2 + (2n - 5)\mathcal{J}] \right. \\ & - \left(\frac{\bar{a}}{\pi L} \right)^3 [\mathcal{I}^3 + (2n - 7)\mathcal{I}\mathcal{J} + (5n^2 - 41n + 63)\mathcal{K}] \\ & + \left(\frac{\bar{a}}{\pi L} \right)^4 [\mathcal{I}^4 - 6\mathcal{I}^2\mathcal{J} + (4 + n - n^2)\mathcal{J}^2 + 4(27 - 15n + n^2)\mathcal{I}\mathcal{K} \\ & \left. + (14n^3 - 227n^2 + 919n - 1043)\mathcal{L}] \right\} \\ & + {}^n C_3 \left[\frac{192 \bar{a}^5}{M\pi^3 L^7} (\mathcal{T}_0 + \mathcal{T}_1 n) + \frac{6\pi \bar{a}^3}{M^3 L^7} (n + 3) \mathcal{I} \right] \\ & + {}^n C_3 \frac{1}{L^6} \frac{\bar{L}}{\bar{\eta}_3} + \mathcal{O}(L^{-8}) \quad , \quad (10) \end{aligned}$$

where the parameter \bar{a} is related to the scattering length⁴, a , and the effective range, r , by

$$a = \bar{a} - \frac{2\pi}{L^3} \bar{a}^3 r \left(1 - \left(\frac{\bar{a}}{\pi L} \right) \mathcal{I} \right) . \quad (11)$$

The geometric constants that enter into eq. (10) are

$$\begin{aligned} \mathcal{I} &= -8.9136329, & \mathcal{J} &= 16.532316, & \mathcal{K} &= 8.4019240, \\ \mathcal{L} &= 6.9458079, & \mathcal{T}_0 &= -4116.2338, & \mathcal{T}_1 &= 450.6392, \end{aligned} \quad (12)$$

and ${}^n C_m = n!/m!(n-m)!$. The three-body contribution to the energy-shift given in eq. (10) is represented by the parameter $\bar{\eta}_3^L$, which is a combination of the volume-dependent, renormalization group invariant quantity, $\bar{\eta}_3^L$, and contributions from the two-body scattering length and effective range,

$$\bar{\eta}_3^L = \bar{\eta}_3^L \left(1 - 6 \left(\frac{\bar{a}}{\pi L} \right) \mathcal{I} \right) + \frac{72\pi \bar{a}^4 r}{ML} \mathcal{I} , \quad (13)$$

where

$$\bar{\eta}_3^L = \eta_3(\mu) + \frac{64\pi a^4}{M} (3\sqrt{3} - 4\pi) \log(\mu L) - \frac{96a^4}{\pi^2 M} \mathcal{S}_{\text{MS}} . \quad (14)$$

The quantity $\eta_3(\mu)$ is the renormalization scale dependent coefficient of the three- π^+ interaction that appears in the effective Hamiltonian density describing the system [8]. The quantity \mathcal{S} is renormalization scheme dependent and its value in the minimal subtraction (MS) scheme is $\mathcal{S}_{\text{MS}} = -185.12506$.

For $n = 2$, the last two terms in eq. (10) vanish and the remaining terms constitute the small \bar{a}/L expansion of the exact eigenvalue equation derived by Lüscher [15, 16],

$$p \cot \delta(p) = \frac{1}{\pi L} \mathbf{S} \left(\left(\frac{pL}{2\pi} \right)^2 \right) , \quad (15)$$

which is valid below the inelastic threshold, where $p \cot \delta(p)$ is the real part of the inverse scattering amplitude. The regulated three-dimensional sum is [15, 16, 17]

$$\mathbf{S}(x) \equiv \sum_{\mathbf{j}}^{\|\mathbf{j}\| < \Lambda} \frac{1}{\|\mathbf{j}\|^2 - x} - 4\pi\Lambda , \quad (16)$$

where the summation is over all triplets of integers \mathbf{j} such that $\|\mathbf{j}\| < \Lambda$ and the limit $\Lambda \rightarrow \infty$ is implicit.

⁴ In this work we use the Nuclear Physics sign convention for the scattering length, opposite to that used in Particle Physics. In this convention, the $\pi^+\pi^+$ scattering length is positive, corresponding to a repulsive interaction.

TABLE I: The parameters of the MILC gauge configurations and domain-wall quark propagators used in this work. The subscript l denotes light quark (up and down), and s denotes the strange quark. The superscript dwf denotes the bare-quark mass for the domain-wall fermion propagator calculation. The last column is the number of configurations times the number of sources per configuration. For the ensembles labeled with “P \pm A”, propagators that were periodic in the temporal direction were computed in addition to those with anti-periodic temporal boundary conditions (bm_{res} was not computed for these sets but is expected to be very close to the result from the corresponding set of propagators with anti-periodic temporal boundary conditions).

Ensemble	bm_l	bm_s	bm_l^{dwf}	bm_s^{dwf}	$10^3 \times bm_{res}$	# of propagators
2064f21b676m007m050	0.007	0.050	0.0081	0.081	1.604	1038×24
2064f21b676m010m050	0.010	0.050	0.0138	0.081	1.552	768×24
2064f21b679m020m050	0.020	0.050	0.0313	0.081	1.239	486×24
2064f21b681m030m050	0.030	0.050	0.0478	0.081	0.982	564×20
2896f2b709m0062m031	0.0062	0.031	0.0080	0.0423	0.380	1001×7
2896f2b709m0062m031 P \pm A	0.0062	0.031	0.0080	0.0423	—	$1001 \times (1+1)$
2864f2b676m010m050	0.010	0.050	0.0138	0.081	1.552	137×8
2864f2b676m010m050 P \pm A	0.010	0.050	0.0138	0.081	—	$274 \times (2+2)$

IV. METHODOLOGY AND DETAILS OF THE LATTICE CALCULATION

The computation in this paper uses the mixed-action lattice QCD scheme developed by LHPC [18, 19] and described fully in Ref. [6] where multi-pion systems are investigated in detail. The present calculations were performed predominantly with the coarse, asqtad-improved [20, 21] MILC configurations generated with rooted staggered sea quarks [22]⁵ with a lattice spacing of $b \sim 0.125$ fm, and a spatial extent of $L \sim 2.5$ fm. These configurations were HYP-smearred [23, 24, 25, 26] and used to generate domain-wall fermion propagators [27, 28, 29, 30, 31]. The strange quark was held fixed near its physical value while the degenerate light quarks were varied over a range of masses⁶; see Table I and Refs. [3, 32, 33, 34, 35] for details. Further calculations were performed using one fine MILC ensemble, with $b \sim 0.090$ fm and $L \sim 2.5$ fm and on a larger volume coarse MILC ensemble with $b \sim 0.125$ fm and $L \sim 3.5$ fm. On the coarse, 2.5 fm MILC lattices, Dirichlet boundary conditions were implemented to reduce the original time extent of 64 time-slices down to 32 and thus save in computational time. While this procedure leads to minimal degradation of baryon signals, it does limit the number of time slices available for fitting meson properties. For the fine MILC ensemble and the large volume coarse MILC ensemble, anti-periodic boundary conditions in time were implemented and all time slices are available for analysis. In order to extract precise measurements from the configurations, propagators were computed from multiple sources displaced both temporally and spatially on each configuration. The correlators were blocked so that one averaged correlator per configuration was used in the subsequent statistical analysis. Further blocking over sets of configurations did not

⁵ The results of this paper assume that the fourth-root trick recovers the correct continuum limit of QCD.

⁶ The mass of the valence quark was chosen to yield a pion mass that matches the pseudo-Goldstone staggered pion [6].

change the resulting uncertainties associated with each observable.

For the fine MILC ensemble and the large volume coarse MILC ensemble, additional propagators were computed using periodic temporal boundary conditions for a subset of the source points. Combining periodic and anti-periodic (in time) propagators from the same source leads to a propagator that is periodic in time over twice the temporal extent of the lattice. These ensembles, labeled “P±A” in Table I, served to explore the effects of temporal boundary conditions.⁷

In order to determine the interaction energy in multi-meson systems, both the single-meson, $C_1(t)$, and n -meson, $C_n(t)$, correlation functions were computed, where t is the Euclidean time separation between the hadronic source and sink operators. For simplicity, meson correlation functions involving only zero-momentum states were calculated. The single-kaon correlation function is

$$C_{K^-}(t) = \sum_{\mathbf{x}} \langle K^+(t, \mathbf{x}) K^-(0, \mathbf{0}) \rangle, \quad (17)$$

where the sum over all spatial sites projects onto the zero-momentum state, $\mathbf{p} = 0$. A correlation function which projects onto the n K^- ground-state is

$$C_{nK^-}(t) = \left\langle \left(\sum_{\mathbf{x}} K^+(t, \mathbf{x}) \right)^n \left(K^-(0, \mathbf{0}) \right)^n \right\rangle, \quad (18)$$

which can be constructed from one light and one strange quark propagator. In eqs. (17) and (18), $K^+(t, \mathbf{x}) = \bar{s}(t, \mathbf{x})\gamma_5 u(t, \mathbf{x})$ is a Gaussian-smearred interpolating field for the charged kaon. In the relatively-large spatial volumes used in the calculation, the interaction energy is a small fraction of the total energy that is dominated by the mass of the kaon. To determine this energy, the ratio of correlation functions,

$$G_{nK^-}(t) \equiv \frac{C_{nK^-}(t)}{[C_{K^-}(t)]^n} \longrightarrow \mathcal{A}_n e^{-\Delta E_{nK} t}, \quad (19)$$

was constructed, with the arrow denoting the large-time, infinite-number-of-gauge-configurations limit (far from the boundary). Due to the (anti-)periodic boundary-conditions imposed on the propagators computed on the fine, and large-volume lattices, the K^- correlation function becomes a single cosh function far from the source, while the n -kaon correlation functions become sums of multiple cosh’s, leading to a non-trivial form for $G_{nK^-}(t)$; further details are given in Appendix A. As an alternative method to calculating the interaction energy (and a check of the systematics), a Jackknife analysis of the difference between the energies extracted from the long-time behavior of the multiple- and single-kaon correlation functions individually was performed, finding results in agreement with those determined from eq. (19). The interaction energy is related to the n -particle energy eigenvalues, E_{nK} , and the kaon mass,

$$\Delta E_{nK} \equiv E_{nK} - n m_K. \quad (20)$$

⁷ For the correlators of systems containing multiple hadrons (which are extremely sensitive to truncation errors in arithmetic operations), we find that performing the P±A additions and subtractions in machine (double) precision leads to mild degradation of signals that worsens with increasing n . This indicates that differences in the iterative (conjugate gradient) propagator inversion for the two types of boundary conditions are becoming significant.

A comprehensive review of the lattice techniques we have used in this work can be found in Refs. [6, 36].

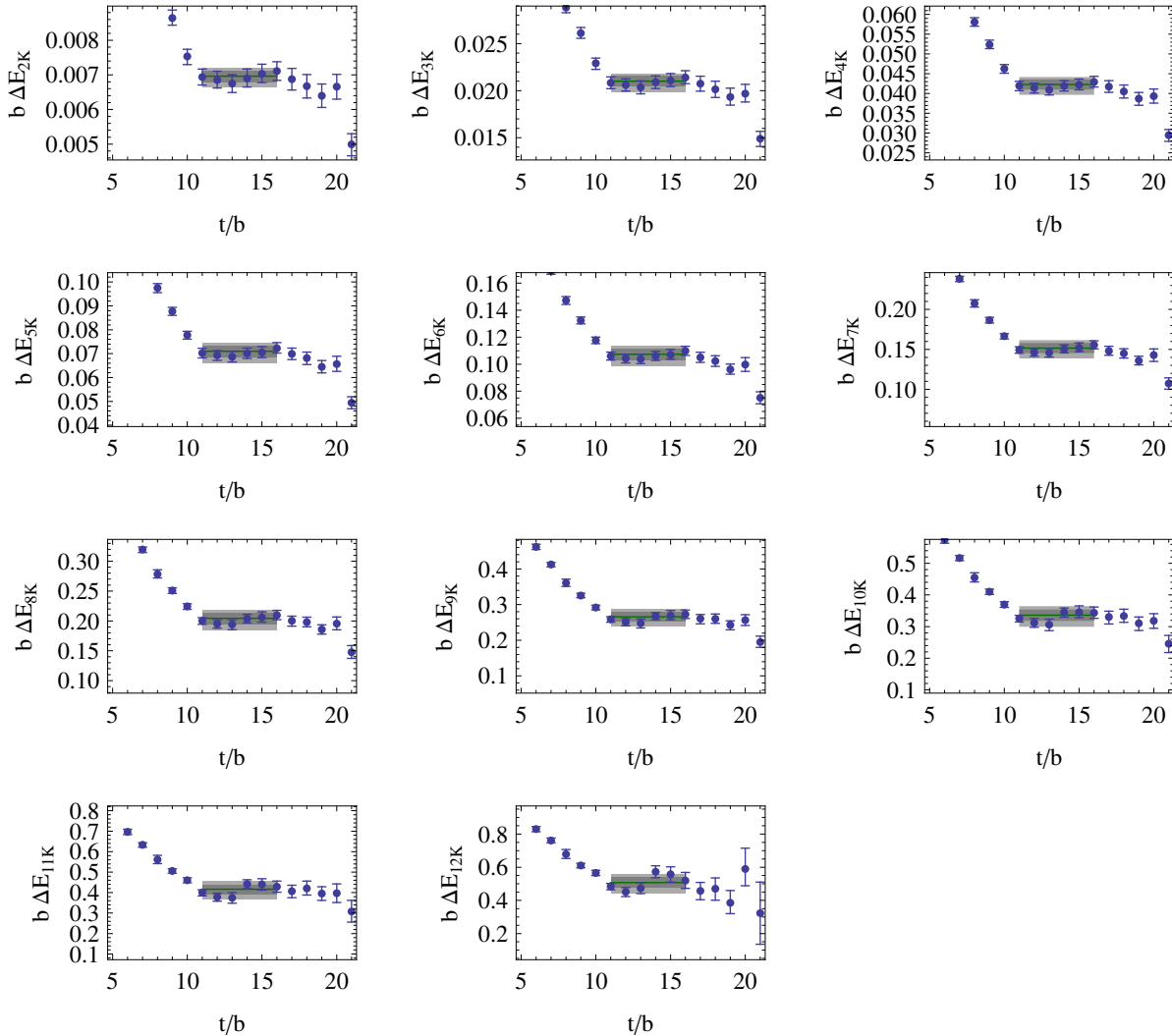


FIG. 1: The energy-differences (in lattice units), $b \Delta E_{nK}$, for the multi-kaon systems with $m_\pi \sim 291$ MeV. The lighter (darker) shaded regions correspond to the statistical and systematic uncertainties combined in quadrature (statistical uncertainty) obtained from fitting the plateau regions. The green line denotes the central value of the fit.

To indicate the quality of the results of this calculation, in fig. 1 we show the effective energy differences, ΔE_{nK} , as defined in eq. (20), for the coarse 2.5 fm ensemble with $m_\pi \sim 291$ MeV. For each n there is clear, multi-time-slice, plateau from which to extract ΔE_{nK} . Figure 1 shows that the systematic uncertainties in the plateau region tend to become more significant as the number of kaons in the system is increased, likely due to the fact that the same propagators are being raised to high powers. In the extraction of ΔE_{nK} from the correlation functions, a correlated χ^2 -fit is performed over the fitting interval. Further, in the extractions of the two- and three- body scattering parameters, correlations among the different ΔE_{nK} are included by performing a coupled n - and t - correlated fit. Systematic uncertainties are assigned to these extractions by varying the ends of the fitting intervals.

It is interesting to note that the uncertainty in the effective n -kaon energy grows with time. This is expected when $m_\pi + m_\phi < 2m_K$ (as is the case for the ensembles studied here) based on the general arguments given in Ref. [37].

V. THREE-MESON INTERACTIONS

The three-meson interactions extracted from our calculations, $m_\pi f_\pi^4 \overline{\eta}_{3\pi^-}^L$ and $m_K f_K^4 \overline{\eta}_{3K^-}^L$, are shown in Fig. 2, in units of the NDA estimate, $\overline{\eta}_{3\pi^-}^{L,(NDA)} = 1/(m_\pi f_\pi^4)$ and $\overline{\eta}_{3K^-}^{L,(NDA)} = 1/(m_K f_K^4)$. Table II contains the extracted values of the two-pion and two-kaon scattering parameters and the three-pion and three-kaon interactions for each ensemble. The results of

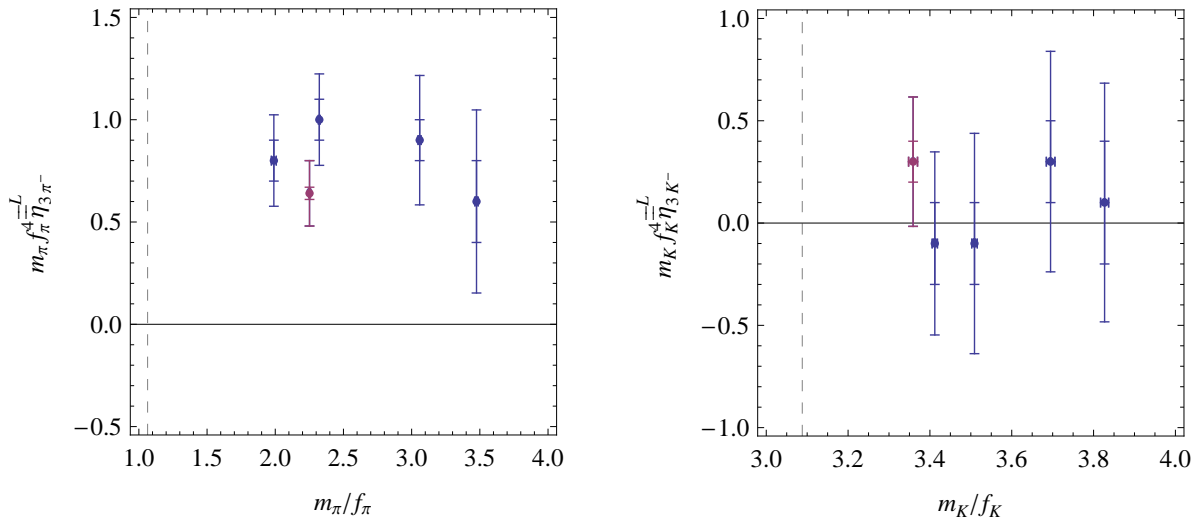


FIG. 2: The three-body interactions, $m_\pi f_\pi^4 \overline{\eta}_{3\pi^-}^L$ and $m_K f_K^4 \overline{\eta}_{3K^-}^L$, defined in eq. (10), as a function of m_π/f_π and m_K/f_K , respectively. The statistical uncertainties and the statistical and systematic uncertainties combined in quadrature are shown as the inner and outer error-bounds, respectively. The dashed vertical lines indicates the physical point.

the calculation of the three-pion interaction on the coarse MILC lattices have been presented previously, and the result from the fine ensemble is consistent with the closest mass coarse results, as can be seen in fig. 2. The three-kaon interaction is found to be consistent with zero for all the kaon masses that have been explored, but the uncertainties are moderately large. This result is consistent with the trend found in multi-pion systems where there is a hint that the three-pion interaction is decreasing with increasing pion mass. As is the case for the three-pion interaction [6], it is not yet possible to extract the RGI three-body interaction, $\overline{\eta}_{3K}^L$ or the underlying parameter $\eta_{3K}(\mu)$ because of the current uncertainties in the calculation. The uncertainties of the three-body interactions measured on the large volume ensemble are significantly larger than those shown in the figure and we do not display them.

TABLE II: Extracted values of the two-body and three-body interactions. Note that $\overline{\eta}_{3\pi^-}^L$ and $\overline{\eta}_{3K^-}^L$ depend on L , eq. (13) and eq. (14) and are quoted at their physical volumes. The systematic uncertainties in the pionic quantities from the coarse $L \sim 2.5$ fm ensembles have been symmetrized about the central value [6]. The pion and kaon scattering lengths obtained on the coarse $L \sim 2.5$ fm ensembles are in agreement with those of Ref. [38, 39], but have slightly smaller uncertainties stemming from increased statistics and from the n -correlated analysis performed here. Quantities extracted from the correlators formed from the $P \pm A$ propagators are consistent with those from the individual propagators.

Ensemble	$m_\pi \overline{a}_{\pi\pi}^{(I=2)}$	$m_\pi f_\pi^4 \overline{\eta}_{3\pi^-}^L$	$m_K \overline{a}_{KK}^{(I=1)}$	$m_K f_K^4 \overline{\eta}_{3K^-}^L$
2064f21b676m007m050	0.164(4)(8)	0.8(1)(2)	0.491(9)(13)	-0.1(2)(4)
2064f21b676m010m050	0.206(5)(6)	1.0(1)(2)	0.503(11)(19)	-0.1(2)(5)
2064f21b679m020m050	0.350(7)(10)	0.9(1)(3)	0.536(10)(19)	0.3(2)(5)
2064f21b681m030m050	0.476(10)(16)	0.6(2)(4)	0.584(12)(18)	0.1(3)(5)
2896f2b709m0062m031	0.178(2)(8)	0.64(3)(16)	0.402(6)(18)	0.3(1)(3)
2864f2b676m010m050	0.25(1)(6)	0(1)(1)	0.52(6)(17)	-5(3)(8)

VI. THE EQUATION OF STATE AND CHEMICAL POTENTIALS

The energy of the n K^- system as a function of volume and of the number of K^- 's is given explicitly in eq. (10) in the large-volume expansion. From the equation of state, the K^- chemical potential is

$$\mu_{K^-} = \left. \frac{dE_{nK}}{dn} \right|_{V=\text{const}}, \quad (21)$$

and can be constructed analytically from eq. (10) or numerically from the results of the lattice calculations by using a simple finite difference approximation. The resulting ratios of the K^- -chemical potentials to the kaon mass on each of the coarse ensembles are shown in Fig. 3 as a function of the K^- -density, ρ_{K^-} in units of $(2.5 \text{ fm})^3$. For comparison Fig. 4 shows the isospin chemical potential computed from the n π^+ systems, expanding upon the results of Ref. [6] by including the large volume coarse ensemble. Finally, Fig. 5 shows the kaon and pion chemical potentials for the fine ensemble, and a comparison between results obtained with anti-periodic boundary conditions and those computed with the $P \pm A$ propagators. We note that for the 12- K^- system, the number density is $\rho_{K^-}^{(12)} = 12/L^3 = 0.77 \text{ fm}^{-3}$ on the ensembles with $L \sim 2.5$ fm. The solid curves in Figs. 3, 4 and 5 correspond to the prediction at $\mathcal{O}(L^{-7})$ from eq. (10) using the extracted two-body and three-body scattering parameters, and differ insignificantly from that at $\mathcal{O}(L^{-6})$. The dotted curves result from setting the three-body interactions to zero.

The results of the lattice QCD calculation are consistent within uncertainties with the prediction of tree-level $SU(3)_L \otimes SU(3)_R$ χ PT which are shown as the dashed lines in Figs. 3, 4 and 5. Given that one expects the tree-level result to be accurate at the $\sim 25\%$ -level, this is quite a remarkable result. The contributions from the higher-order counterterms and loop diagrams have conspired to produce a shift from tree-level that is much less than one expects from NDA.

In comparing these lattice QCD calculations of the chemical potential to those calculated

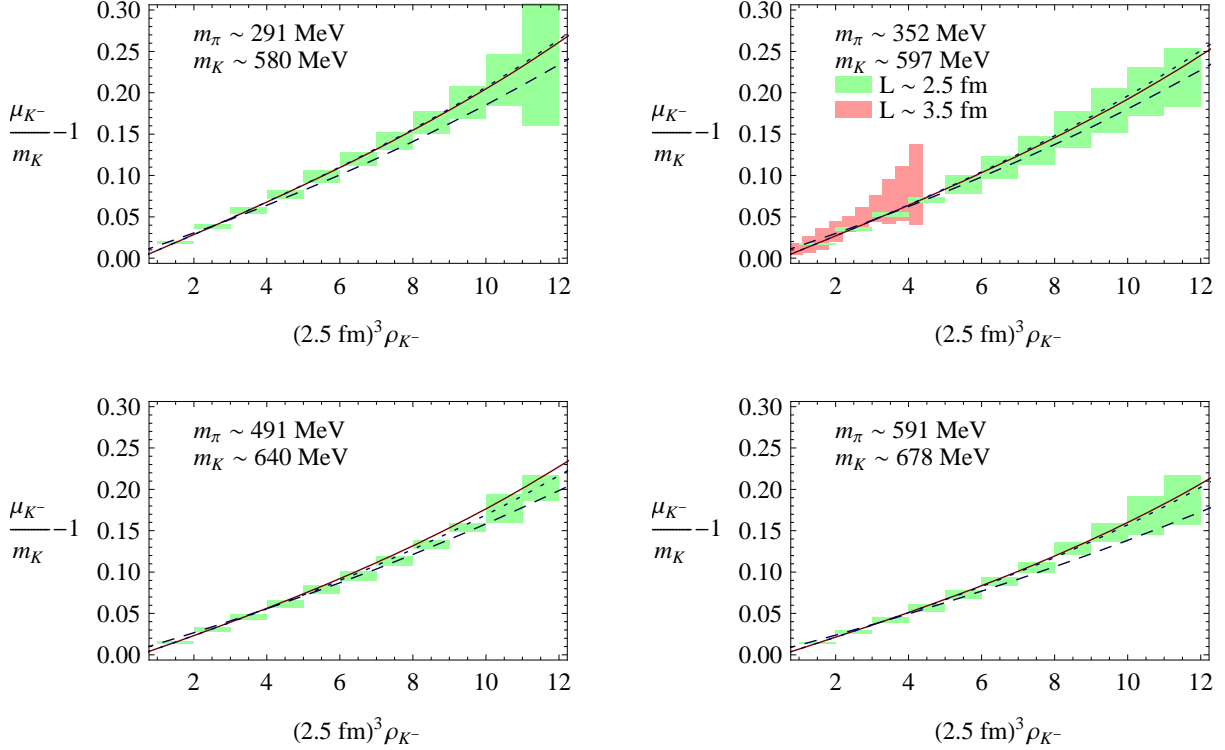


FIG. 3: The K^- chemical potential, μ_{K^-} , as a function of the density of K^- 's on the coarse MILC lattices. The rectangular regions are the results of the lattice calculation where a finite-difference has been used to construct the derivative with respect to the number of K^- 's. The lighter (green) rectangles are obtained from the lattices with spatial extent $L \sim 2.5 \text{ fm}$, while the darker (red) rectangles are obtained from the lattices with $L \sim 3.5 \text{ fm}$. The dashed curves correspond to tree-level χ PT. The darker solid curve corresponds to the analytic expression for the energy of the ground state in the large volume expansion, eq. (10), using the fit values for $\bar{a}_{KK}^{(I=1)}$ and $\bar{\eta}_{3K^-}^L$. The lighter dotted curve shows the analytic forms with the fit value of $\bar{a}_{KK}^{(I=1)}$ but with $\bar{\eta}_{3K^-}^L$ set to zero.

in χ PT in Section II, we note that they are performed in finite volumes and at non-vanishing lattice spacings. These approximations modify the chemical potential expected in the lattice calculation from chiral perturbation theory at most at NLO in the chiral expansion. The fact that LO χ PT is in good agreement with our numerical results, on both the larger and smaller volume coarse ensembles and the fine ensemble, suggests that finite volume and lattice spacing effects are small. For $m_\pi \sim 352 \text{ MeV}$, the two calculations at different volumes agree within their uncertainties, also supporting this claim.

VII. CONCLUSIONS

Kaon condensation may play an important role in the evolution of supernovae [1]. The theoretical analysis of the condensation mechanism presently relies upon chiral perturbation theory to determine both the interactions of kaons with the baryonic matter and the kaon

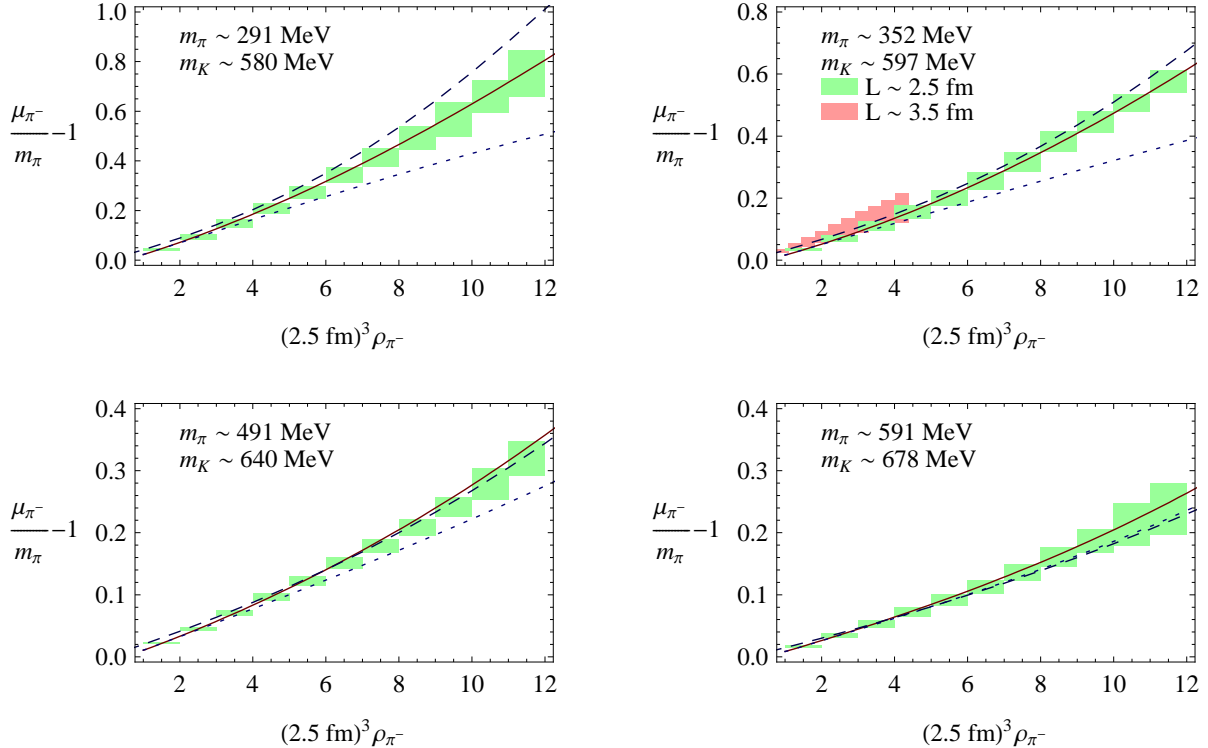


FIG. 4: The isospin-chemical potential, μ_I , as a function of the density of π^- 's on the coarse MILC lattices. The rectangular regions are the results of the lattice calculation where a finite-difference has been used to construct the derivative with respect to the number of π^- 's. The lighter (green) rectangles are obtained from the lattices with spatial extent $L \sim 2.5$ fm, while the darker (red) rectangles are obtained from the lattices with $L \sim 3.5$ fm. The dashed curves correspond to tree-level χ PT. The darker solid curve corresponds to the analytic expression for the energy of the ground state in the large volume expansion, eq. (10), using the fit values for $\bar{a}_{\pi\pi}^{(I=2)}$ and $\bar{\eta}_{3\pi}^L$. The lighter dotted curve shows the analytic forms with the fit value of $\bar{a}_{\pi\pi}^{(I=2)}$ but with $\bar{\eta}_{3\pi}^L$ set to zero.

self-interactions. We have performed the first Lattice QCD investigation of the charged kaon condensate, isolating part of the mechanism that may be in action in the interior of neutron stars. In particular, we have explored the K^- chemical potential as a function of density. We have also updated our previous analysis of the charged pion condensate. Surprisingly, LO χ PT is found to reproduce the results of the Lattice QCD calculations to within the uncertainties of the calculation. This is significantly better than the $\sim 25\%$ -level expected from dimensional analysis. However, this is consistent with the findings of other lattice calculations that higher orders in chiral perturbation theory make contributions that are much smaller than naively expected, e.g. Ref. [36], in this range of meson masses.

To move toward exploring the possibility of kaon condensation in a baryonic background, lattice calculations of systems containing multiple nucleons and multiple kaons will be required. Only one dynamical lattice QCD calculation of the two-nucleon system has been performed to date [32], and exploration of the multi-nucleon-multi-kaon systems are left for

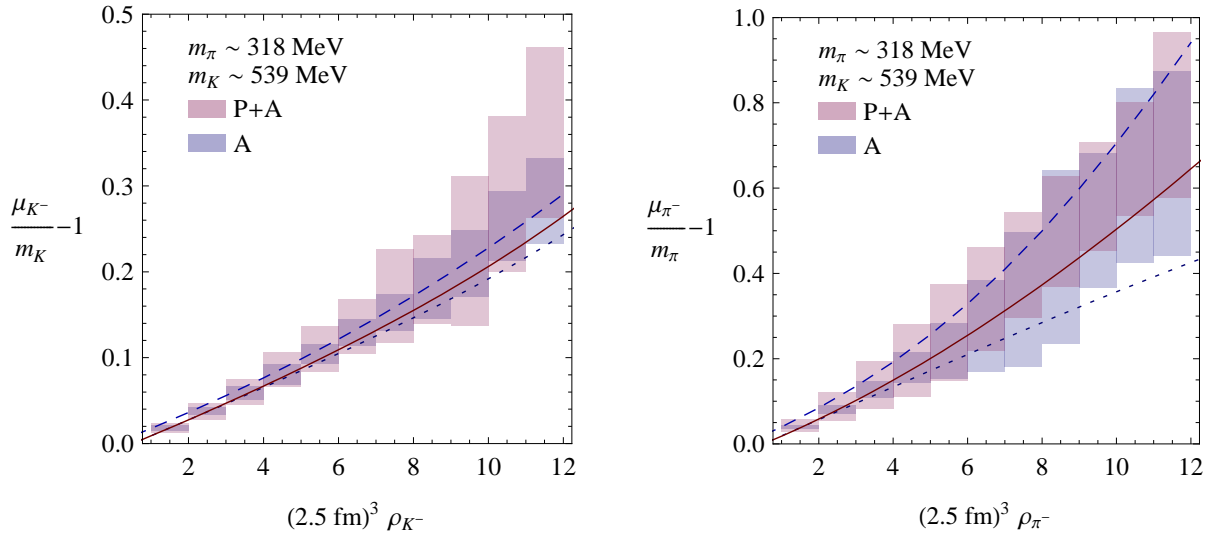


FIG. 5: The K^- chemical potential, μ_{K^-} , as a function of the density of K^- 's on the fine MILC lattice ensemble (left panel) and the isospin chemical potential, μ_I as a function of the density of π^+ 's on the same ensemble (right panel). The rectangular regions show the results of the lattice calculation where a finite-difference has been used to construct the derivative with respect to the density of mesons. The lighter (blue) rectangles are obtained from purely anti-periodic temporal boundary conditions on the quark propagators, while the darker (purple) rectangles are obtained from the P \pm A propagators. The dashed curves correspond to LO χ PT. The darker solid curve corresponds to the analytic expressions for the energy of the ground state in the large volume expansion, eq. (10), using the fit values of the two-body and three-body interactions. The lighter dotted curve shows the analytic forms with the fit value of the two-body interaction but with three-body interactions set to zero.

the future. In addition to the increased exponential degradation of the signal-to-noise ratio associated with baryonic correlation functions [37], “disconnected diagrams” (in which a quark is created and annihilated at the source) will contribute to the multi-nucleon-multi- K^- correlation functions, and therefore the computational resources required to perform such calculations will be considerably larger than currently available for the study of multi-hadron systems.

VIII. ACKNOWLEDGMENTS

We thank Silas Beane, Tom Luu, Assumpta Parreño and Aaron Torok for contributing to the quark propagator calculations required for this work. We thank Michael Endres and Steve Sharpe for discussions, and R. Edwards and B. Joo for help with the QDP++/Chroma programming environment [40] with which the propagator calculations discussed here were performed. The computations for this work were performed at Jefferson Lab, Fermilab, Centro Nacional de Supercomputación (Barcelona, Spain), the University of Washington and the National Energy Research Scientific Computing Center, which is supported by the Office of

Science of the U.S. Department of Energy under Contract No. DE-AC02-05CH11231. This research was also supported in part by the National Science Foundation through TeraGrid resources provided by the National Center for Supercomputing Applications. We are indebted to the MILC for use of their configurations. The work of MJS and WD was supported in part by the U.S. Dept. of Energy under Grant No. DE-FG03-97ER4014. The work of KO was supported in part by the U.S. Dept. of Energy contract No. DE-AC05-06OR23177 (JSA) and by the Jeffress Memorial Trust, grant J-813, DOE OJI grant DE-FG02-07ER41527 and DOE grant DE-FG02-04ER41302. The work of AW-L was supported in part by DOE OJI grant DE-FG02-07ER41527 and DOE grant DE-FG02-93ER40762.

APPENDIX A: EFFECTS OF TEMPORAL BOUNDARIES

For temporally periodic gauge configurations and (anti-) periodic quark propagators (or the $P\pm A$ propagators), we are in a position to account for the effects of the temporal boundary condition. As is well known, a single meson correlation function, generated from propagators that are subject to periodic or anti-periodic boundary conditions, does not decay exponentially but is periodic in time and is given by the sum of forward and backward propagating exponentials, leading to the behavior

$$C_1(t) \xrightarrow{t \gg 1} A_1 [e^{-E_1 t} + e^{-E_1(T-t)}] , \quad (\text{A1})$$

where T is the temporal period and the source is defined to be at $t = 0$. For a two meson correlation function, there are two contributions; the two mesons can propagate either forward or backward or one meson can propagate forward and one backward. This leads to a correlator

$$C_2(t) \xrightarrow{t \gg 1} A_2 [e^{-E_2 t} + e^{-E_2(T-t)}] + B_{1,1} , \quad (\text{A2})$$

where the second term is t independent as it is a product of $\exp[-E_1 t]$ and $\exp[-E_1(T-t)]$. This can further be extended to the n meson case, where the n -meson correlation function is given by

$$C_n(t) \xrightarrow{t \gg 1} A_n [e^{-E_n t} + e^{-E_n(T-t)}] + \sum_{m=1}^{\lfloor \frac{n}{2} \rfloor} B_{n,m} [e^{-E_{n-m} t} e^{-E_m(T-t)} + e^{-E_m t} e^{-E_{n-m}(T-t)}] . \quad (\text{A3})$$

We have used the fact that a positive definite transfer matrix guarantees that the energies occurring in these expressions do not depend on the correlator they appear in, although the normalizations $B_{i,j}$ do. This is only true over physical length scales for the DW fermion discretization used herein.

In principle, these expressions can be used to extract the energies, E_1, \dots, E_{12} from the measured correlations. However, there are increasing numbers of parameters to determine as n increases (e.g., $n = 12$ involves eight new parameters) and we have only been able to successfully perform this analysis up to $n = 6$. The energies determined with this procedure are consistent with those extracted from the plateaus in the effective mass plots of the individual correlation functions, but with somewhat larger uncertainties.

As a further check of our primary analysis, the correlators generated by combining the propagators subject to periodic boundary conditions with those subject to anti-periodic

boundary conditions, denoted by $P\pm A$, (whose behaviors are described by eqs. (A1), (A2) and (A3) in which T is replaced by $2T$, significantly reducing the contributions of backward propagating states) were compared with the corresponding correlation functions using only anti-periodic boundary conditions for the quark propagators. On both the fine and large volume coarse MILC ensembles, statistical agreement was found for the extracted n - π and n - K energies for all n studied. Fig. 5 compares the two extractions of the π^- and K^- chemical potentials for the fine ensemble.

In the case of a Dirichlet boundary in time, as employed in the calculation of quark propagators on the coarse $L \sim 2.5$ fm ensembles, the nature of the states reflected from the walls is less clear and we do not attempt to account for them, instead restricting our analysis to a region that is well separated from the walls.

-
- [1] G. E. Brown and H. Bethe, *Astrophys. J.* **423**, 659 (1994).
 - [2] D. Page and S. Reddy, *Ann. Rev. Nucl. Part. Sci.* **56**, 327 (2006) [arXiv:astro-ph/0608360].
 - [3] S. R. Beane, P. F. Bedaque, T. C. Luu, K. Orginos, E. Pallante, A. Parreño and M. J. Savage [NPLQCD Collaboration], *Nucl. Phys. A* **794**, 62 (2007) [arXiv:hep-lat/0612026].
 - [4] D. B. Kaplan and A. E. Nelson, preprint HUTP-86/A023; *Phys. Lett. B* **175** (1986) 57; *Phys. Lett. B* **192**, 193 (1987); *Nucl. Phys. A* **479**, 273 (1988); *Nucl. Phys. A* **479**, 285 (1988); *IN *BERKELEY 1986, PROCEEDINGS, HIGH ENERGY PHYSICS, VOL. 2* 1430-1432*.
 - [5] S. R. Beane, W. Detmold, T. C. Luu, K. Orginos, M. J. Savage and A. Torok, *Phys. Rev. Lett.* **100**, 082004 (2008) [arXiv:0710.1827 [hep-lat]].
 - [6] W. Detmold, M. J. Savage, A. Torok, S. R. Beane, T. C. Luu, K. Orginos and A. Parreño, arXiv:0803.2728 [hep-lat] to appear in *Phys. Rev. D*.
 - [7] S. R. Beane, W. Detmold and M. J. Savage, *Phys. Rev. D* **76**, 074507 (2007) [arXiv:0707.1670 [hep-lat]].
 - [8] W. Detmold and M. J. Savage, *Phys. Rev. D* **77**, 057502 (2008) [arXiv:0801.0763 [hep-lat]].
 - [9] D. T. Son and M. A. Stephanov, *Phys. Rev. Lett.* **86**, 592 (2001) [arXiv:hep-ph/0005225].
 - [10] D. T. Son and M. A. Stephanov, *Phys. Atom. Nucl.* **64**, 834 (2001) [*Yad. Fiz.* **64**, 899 (2001)] [arXiv:hep-ph/0011365].
 - [11] J. B. Kogut and D. Toublan, *Phys. Rev. D* **64**, 034007 (2001) [arXiv:hep-ph/0103271].
 - [12] S. Tan, arXiv:0709.2530 [cond-mat.stat-mech].
 - [13] N. N. Bogoliubov, *J. Phys. (Moscow)* **11**, 23 (1947).
 - [14] T. D. Lee, K. Huang, and C. N. Yang, *Phys. Rev.* **106**, 1135 (1957)
 - [15] M. Lüscher, *Commun. Math. Phys.* **105**, 153 (1986).
 - [16] M. Lüscher, *Nucl. Phys. B* **354**, 531 (1991).
 - [17] S. R. Beane, P. F. Bedaque, A. Parreño and M. J. Savage, *Phys. Lett. B* **585**, 106 (2004) [arXiv:hep-lat/0312004].
 - [18] D. B. Renner *et al.*, *Nucl. Phys. Proc. Suppl.* **140**, 255 (2005).
 - [19] R. G. Edwards *et al.*, *PoS LAT2005*, 056 (2005).
 - [20] K. Orginos, D. Toussaint and R. L. Sugar, *Phys. Rev. D* **60**, 054503 (1999).
 - [21] K. Orginos and D. Toussaint, *Phys. Rev. D* **59**, 014501 (1999).
 - [22] C. W. Bernard *et al.*, *Phys. Rev. D* **64**, 054506 (2001).
 - [23] A. Hasenfratz and F. Knechtli, *Phys. Rev. D* **64**, 034504 (2001).
 - [24] T. A. DeGrand, A. Hasenfratz and T. G. Kovacs, *Phys. Rev. D* **67**, 054501 (2003).

- [25] T. A. DeGrand, Phys. Rev. D **69**, 014504 (2004).
- [26] S. Dürr, C. Hoelbling and U. Wenger, Phys. Rev. D **70**, 094502 (2004).
- [27] D. B. Kaplan, Phys. Lett. B **288**, 342 (1992) [arXiv:hep-lat/9206013].
- [28] Y. Shamir, Phys. Lett. B **305**, 357 (1993) [arXiv:hep-lat/9212010].
- [29] Y. Shamir, Nucl. Phys. B **406**, 90 (1993) [arXiv:hep-lat/9303005].
- [30] V. Furman and Y. Shamir, Nucl. Phys. B **439**, 54 (1995) [arXiv:hep-lat/9405004].
- [31] Y. Shamir, Phys. Rev. D **59**, 054506 (1999) [arXiv:hep-lat/9807012].
- [32] S. R. Beane, P. F. Bedaque, K. Orginos and M. J. Savage, Phys. Rev. Lett. **97**, 012001 (2006) [arXiv:hep-lat/0602010].
- [33] S. R. Beane, K. Orginos and M. J. Savage, Phys. Lett. B **654**, 20 (2007) [arXiv:hep-lat/0604013].
- [34] S. R. Beane, K. Orginos and M. J. Savage, Nucl. Phys. B **768**, 38 (2007) [arXiv:hep-lat/0605014].
- [35] S. R. Beane, P. F. Bedaque, K. Orginos and M. J. Savage, Phys. Rev. D **75**, 094501 (2007) [arXiv:hep-lat/0606023].
- [36] S.R. Beane, K. Orginos and M. J. Savage, arXiv:0805.4629 [hep-lat].
- [37] G. P. Lepage, ‘‘The Analysis Of Algorithms For Lattice Field Theory,’’ Invited lectures given at TASI’89 Summer School, Boulder, CO, Jun 4-30, 1989. Published in Boulder ASI 1989:97-120 (QCD161:T45:1989).
- [38] S. R. Beane, T. C. Luu, K. Orginos, A. Parreno, M. J. Savage, A. Torok and A. Walker-Loud [NPLQCD Collaboration], Phys. Rev. D **77**, 094507 (2008) [arXiv:0709.1169 [hep-lat]].
- [39] S. R. Beane, T. C. Luu, K. Orginos, A. Parreno, M. J. Savage, A. Torok and A. Walker-Loud, Phys. Rev. D **77**, 014505 (2008) [arXiv:0706.3026 [hep-lat]].
- [40] R. G. Edwards and B. Joo [SciDAC Collaboration], Nucl. Phys. Proc. Suppl. **140** (2005) 832 [arXiv:hep-lat/0409003].